Model predictive control based on the generalized Bouc-Wen model for piezoelectric actuators in robotic hand with only position measurements

Gerardo Flores, *Member, IEEE*, Noé Aldana, and Micky Rakotondrabe, *Member, IEEE*

***Abstract*— Hysteresis nonlinearity is known to typify piezoelectric actuators and systems. If not appropriately accounted for in the control law, it can lead to the closed-loop's performance loss or even instability. Several studies have proposed various techniques to design control laws with explicit consideration of this nonlinearity. However, they are limited to symmetrical hysteresis, and their efficiency is no longer ensured in the face of asymmetrical ones. This paper proposes to model the strong asymmetrical hysteresis in a piezoelectric actuator devoted to robotic hands using the generalized Bouc-Wen model. A Hammerstein structure is employed to also account for its dynamics. Then, we propose an output feedback control law consisting of nonlinear control and a nonlinear model predictive control. To get an estimate of the hysteresis signal used for feedback, we design a nonlinear observer. The observer and controls together stabilize the closed-loop output. The efficiency of the proposed control technique is finally demonstrated through several simulations.**

***Index Terms*— Generalized Bouc-Wen model, hysteresis control, model predictive control, observer, piezoelectric system, robot hand.**

I. Introduction

In applications that generally require precise positioning (sub-micrometer) like medical microrobotics, hard-disk drives, and scanning probe microscopy, smart materials-based actuators are widely used. Such actuators minimize mechanical play, which is one of the principal sources of imprecision and which is often found in poly-articulated positioning systems based on DC motors like standard robots and standard robotic hands [1]. Among these smart materials-based actuators, piezoelectric ones are the most used [2]–[6]. This recognition on piezoelectric actuators is mainly thanks to the high resolution they can offer, since a motion of some nanometer can be obtained. Moreover, they have high bandwidth: some hundreds of Hertz for certain piezoelectric actuators while several kiloHertz for others. Besides, the fact that they are supplied directly with electricity makes them easy to integrate and to design new instruments, contrary to thermal-based actuators or fluidic ones [1].

Manuscript received September 15, 2021; revised November 18, 2021; accepted December 13, 2021. Date of publication XXX, 202X; date of current version XXX, 202X. Recommended by Senior Editor G. Cherubini.

G. Flores and N. Aldana are with the Laboratorio de Percepción y Robótica (LAPyR), Center for Research in Optics, Loma del Bosque 115, León, Guanajuato, 37150 Mexico (Corresponding author e-mail: gflores@cio.mx).

Micky Rakotondrabe is with the Laboratoire Génie de Production, National School of Engineering in Tarbes (ENIT - INPT), University of Toulouse, Tarbes, France. (e-mail: mrakoton@enit.fr).

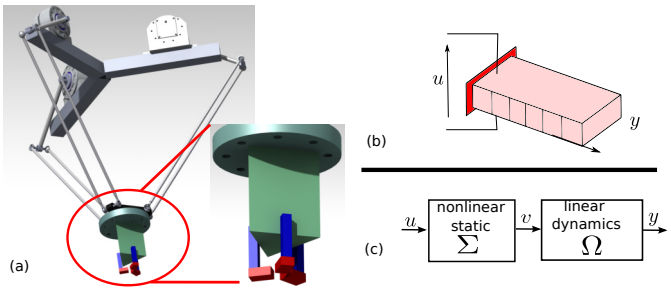

Fig. 1: (a): parallel robotic platform and robotic hand with three fingers. (b): one piezoelectric actuator as a finger. (c): Hammerstein structure.

Within a current project which consists in introducing to a parallel robot additional capacity to manipulate objects (Fig. 1-a), we use three piezoelectric actuators as fingers. Each of the three actuators is supplied by a voltage u allowing it to elongate along the y-axis (Fig. 1-b). Appropriate and synchronized voltages applied to the three actuators allow to close the robotic hand, pick an object and finely move the latter. This slight motion can be used as complementary to that of the robot itself during the insertion of the object inside another one.

Though the above advantages, piezoelectric actuators exhibit nonlinearities (creep and hysteresis) which undeniably degrade the systems' precision performance, or even the stability, if not appropriately accounted for. Moreover, certain structures of piezoelectric actuators are typified by poorly damped vibrations that increase the overall settling time if not controlled.

The control of the hysteresis phenomenon in piezoelectric actuators has raised several studies in the literature. They can be categorized into feedforward (without feedback sensor) and feedback architectures. The principle of feedforward control

architecture consists of modeling as precisely as possible the hysteresis phenomenon and then computing and putting the inverse (or an approximate of the inverse) of the model in cascade with the actual actuator. The inverse model serves, therefore, as a hysteresis compensator. The models used in this approach can be classified into differential models, mainly the Bouc-Wen modeling techniques [7], [8], and into operator-based modeling techniques, mainly the Prandtl-Ishlinskii models [9], [10] and the Preisach models [11], [12]. An advantage of feedforward architecture is the *low-cost* implementation since no sensor is used. Moreover, this architecture is appreciated in processes where it is impossible to implement sensors or where there is a lack of appropriate sensors, such as in microsystems [1]. However, in counterpart, feedforward architecture is known for its lack of robustness. Several controller designs have been studied in feedback control architecture. They can be categorized into model based control [13]–[16] and non-model based control [17]. The main advantage of model-based control is that one knows about the system's hysteresis and exploits its model to design the control law. As a result, this can provide better performances than with non-model-based control. Our recent work proposed a model-based control technique for a piezoelectric actuator devoted to the above robotic hand. The controller was synthesized based on the classical Bouc-Wen model of hysteresis and completed with a nonlinear observer. However, the classical Bouc-Wen model of hysteresis is only valid for symmetrical hysteresis. Though it was observed that piezoelectric actuators could exhibit strong asymmetry properties in their hysteresis behavior (see for instance [7]), which, if not properly accounted for, could drastically lead to feedback instability. Therefore, it is obvious that accounting for such asymmetry in the modeling will further help design a proper controller to ensure stability or even specified performances.

This paper proposes a control law for a piezoelectric actuator devoted to a robotic hand and exhibiting strong asymmetrical hysteresis. We consider the creep and the badly damped vibrations already feedforward controlled using techniques in [18] and [19], respectively. Instead of using the classical Bouc-Wen model, we use the generalized Bouc-Wen model to account for the hysteresis asymmetry. Moreover, we assume that only the displacement generated by the piezoelectric actuator (i.e., position) is available for measurement. Thus, we propose a nonlinear observer to estimate both the hysteresis state and the process (dynamics) state. Finally, based on the estimated state and the measured position, we design a desired hysteresis h_d serving as a virtual control for the disturbed linear part of the system. A nonlinear model predictive control is synthesized to track h_d, optimizing the control law for better tracking performances.

In the sequel, section-II presents the problem statement and the generalized Bouc-Wen model. Section-III details the design of the observer. Section-IV presents the control law including the nonlinear model predictive control, while section-V gives for simulation results. Concluding remarks and perspectives are presented in section-VI.

II. Problem setting

To represent the strong asymmetrical hysteresis nonlinearity of the piezoelectric actuator devoted to the robotic hand, we use *the generalized Bouc-Wen model*. This model extends the classical Bouc-Wen model of hysteresis we employed in our previous work and is limited to symmetrical hysteresis [16]. We highlight that both models are static, i.e., the hysteresis behavior they represent is static [7], [8]. Hence, to account for the dynamics of the actuator, we propose to employ the Hammerstein structure as depicted in Fig. 1-c (e.g. [16]). In this, the static nonlinearity Σ is the hysteresis and is followed by a linear dynamics Ω, where v is an intermediary signal. This representation is motivated by the fact that hysteresis in piezoelectric actuators is due to the electromechanical transduction and has very high dynamics ($20kHz$ or more) such that it can be considered as static. In contrast, the mechanical part has slow and thus dominant dynamics (around or less than the kiloHertz) [1]. To summarize, the model to be used is:

$$\Sigma : \begin{cases} v = d_p u - h \\ \dot{h} = \dot{u}\left(\alpha - |h|^m \Phi(u,\dot{u},h)\right) + \delta_h(t) \\ \Phi(u,\dot{u},h) = \beta_1 \operatorname{sgn}(\dot{u}h) + \beta_2 \operatorname{sgn}(\dot{u}u) \\ \qquad\qquad +\beta_3 \operatorname{sgn}(uh) + \beta_4 \operatorname{sgn}(\dot{u}) \\ \qquad\qquad\quad +\beta_5 \operatorname{sgn}(h) + \beta_6 \operatorname{sgn}(u) \end{cases} \tag{1}$$

$$\Omega : \begin{cases} \dot{x} = Ax + Bv + \delta_x(t) \\ y = Cx \end{cases} \tag{2}$$

where:

- the generalized Bouc-Wen model Σ is characterized by an internal hysteresis state h and contains two equations: a linear *output* equation (equation of the intermediary signal v), and a nonlinear differential state equation (governing model of h). Parameter d_p provides a general slope of the hysteresis, while parameters m and β_i ($i = 1 \rightarrow 6$) indicate its width and asymmetry level [7]. For the piezoelectric actuator studied in this paper, it was shown that $m = 1$, [7].
- the linear dynamics Ω is characterized by an internal state x and described by the realization $(A, B, C, 0)$,
- a state disturbance δ_x is considered acting on the linear dynamics, while disturbance δ_h captures the unmodeled dynamics.

The problem studied in this paper will be:

Problem. *Consider the system described by Fig. 1-c with the model Σ in* (1) *and Ω in* (2)*. The available signals are only the voltage u and the position y. The problem consists in finding a control law to stabilize the state $y(t)$ to a desired trajectory $y_d(t)$ despite the unknown terms $(\delta_h(t), \delta_x(t))$.*

We study an output-feedback control structure because of the limited available signals to (u, y). Therefore, we suggest designing an observer for estimating the states (x, h) to control the system (Σ, Ω), [20], [21].

III. Observer

We aim to use the hysteresis h in Ω as a virtual control input to stabilize x to the desired value y_d. Thus, it is required to

get estimates of the unavailable state h in the system Σ.

Considering the above, we design a hysteresis observer designed in the following. Let us begin by studying the observability of the system Σ.

Lemma 1. *Assuming that $B \neq 0$, the system (Σ, Ω) is observable.*

Proof. Notice that we can arrange the system (Σ, Ω) as follows

$$\begin{aligned} \dot{z} &= \Gamma z + g(z, u, \dot{u}) + \varphi(u, \dot{u}) + \delta(t) \\ y &= \bar{C} z \end{aligned} \tag{3}$$

where $z = [z_1,\ z_2]^\intercal = [x,\ h]^\intercal$, the unknown vector due to unmodeled terms and external disturbances is $\delta(t) = [\delta_x, \delta_h]^\intercal$, the output vector is $\bar{C} = [1, 0]$, and $\varphi(u, \dot{u}) = [B d_p u,\ \alpha \dot{u}]^\intercal$,

$$\Gamma = \begin{pmatrix} A & -B \\ 0 & 0 \end{pmatrix}, \quad g(\cdot) = \begin{pmatrix} 0 \\ -\dot{u}|h|^m \Phi(u, \dot{u}, h) \end{pmatrix}. \tag{4}$$

Then, since $\operatorname{rank} \mathcal{O} = 2$, where $\mathcal{O} = \begin{pmatrix} \bar{C} \\ \bar{C}\Gamma \end{pmatrix}$ is the observability matrix, the system (Σ, Ω) is observable as long as $B \neq 0$. □

For the design of an observer of the system (Σ, Ω) given by (3), let us consider the following assumptions.

Assumption 1. *The control input $u(t)$ and its time-derivative $\dot{u}(t)$ are bounded.*

Assumption 2. *The disturbance vector $\delta(t) = [\delta_x, \delta_h]^\intercal$ in* (3) *is bounded by $\|\delta\|_2 \leq \varrho \|\epsilon\|_2$, where $\epsilon = \hat{z} - z$ is the observation error, and $\|\cdot\|_2$ is the Euclidean norm.*

The observer is given in the following proposition.

Proposition 1. *Consider Assumptions 1 and 2 and let S the solution of the following Lyapunov-like equation*

$$\theta S + \Gamma^\intercal S + S\Gamma - C^\intercal C = 0, \tag{5}$$

where θ is a positive real number, then, the observer

$$\begin{aligned} \dot{\hat{z}} = \Gamma \hat{z} + g(\hat{z}, u, \dot{u}) + \varphi(u, \dot{u}) \\ - S^{-1} C^\intercal C \epsilon - k S^{-1} C^\intercal C \operatorname{Sgn}(\epsilon) \end{aligned} \tag{6}$$

where $k \in \mathbb{R}_{>0}$, $\operatorname{Sgn} \epsilon = \begin{pmatrix} \operatorname{sgn} \epsilon_1 \\ \operatorname{sgn} \epsilon_2 \end{pmatrix}$, stabilizes the origin $\epsilon = [\epsilon_1, \epsilon_2]^\intercal = \hat{z} - z$ in finite time.

Proof. Let us define the observer error as $\epsilon = \hat{z} - z$, whose time-derivative is

$$\begin{aligned} \dot{\epsilon} = \Gamma \epsilon + g(\hat{z}, u, \dot{u}) - g(z, u, \dot{u}) - S^{-1} C^\intercal C \epsilon \\ - k S^{-1} C^\intercal C \operatorname{Sgn}(\epsilon) - \delta(t). \end{aligned} \tag{7}$$

It is possible to get a solution of (5) by simple calculations. This is given by, $S = \begin{pmatrix} s_{1,1} & s_{1,2} \\ s_{2,1} & s_{2,2} \end{pmatrix}$, where $s_{1,1} = \frac{1}{2A+\theta}$, $s_{1,2} = s_{2,1} = \frac{B}{(2A+\theta)(A+\theta)}$, and $s_{2,2} = \frac{2B^2}{(\theta)(2A+\theta)(A+\theta)}$. The matrix S results to be a symmetric positive definite matrix as long as $\theta \in \mathbb{R}_{>0}$ and $\theta > 2A$, since with these values the leading principal minors of S are positive.

Now, let us consider the candidate Lyapunov function $V = \frac{1}{2}\epsilon^\intercal S \epsilon$ whose time-derivative along the solutions of the error system (7) is given by

$$\begin{aligned} \dot{V} = \epsilon^\intercal S \Big(\Gamma \epsilon + g(\hat{z}, \dot{u}) - g(z, \dot{u}) - S^{-1} C^\intercal C \epsilon \\ - k S^{-1} C^\intercal C \operatorname{Sgn} \epsilon - \delta(t) \Big) \\ \leq \epsilon^\intercal S \Gamma \epsilon + \|\epsilon\| \|S\| \|g(\hat{z}, \dot{u}) - g(z, \dot{u})\| \\ - \epsilon^\intercal C^\intercal C \epsilon - k|\epsilon_1| + \|\epsilon\| \|S\| \|\delta(t)\|. \end{aligned} \tag{8}$$

Notice that $g(\cdot)$ in (4) is not Lipschitz. However, we take into account Assumption 1 and the fact that in piezoelectric actuators the hysteresis is assumed to be bounded. And from $\Phi(u, \dot{u}, h)$ in subsystem Σ, it follows that $g(\cdot)$ is also bounded, i.e., $\|g(z, u, \dot{u})\| \leq \gamma |\dot{u}|_\infty |h|_\infty^m = \sigma$, where $\gamma = \sum_{i=0}^{6} |\beta_i|$, and $\sigma \in \mathbb{R}_{>0}$. And thus,

$$\begin{aligned} \|g(\hat{z}, u, \dot{u}) - g(z, u, \dot{u})\| &\leq \gamma |\dot{u}|_\infty \|\hat{|h|}^m - |h|^m\| \\ &\leq \gamma |\dot{u}|_\infty \|\hat{h}^m - h^m\| \leq \gamma |\dot{u}|_\infty |\epsilon_2| \end{aligned} \tag{9}$$

which holds from the reverse triangle inequality, since $m = 1$. Then,

$$\begin{aligned} \dot{V} \leq -\epsilon^\intercal \left(-S\Gamma + C^\intercal C \right) \epsilon + \gamma \|S\| \|\epsilon\| |\dot{u}|_\infty |\epsilon_2| \\ - k|\epsilon_1| + \|\epsilon\| \|S\| \|\delta(t)\|. \end{aligned} \tag{10}$$

Thus,

$$\begin{aligned} \dot{V} \leq -\epsilon^\intercal \left(\theta S + \Gamma^\intercal S \right) \epsilon + \gamma \|S\| |\dot{u}|_\infty |\epsilon_2| \left(|\epsilon_1| + |\epsilon_2| \right) \\ - k|\epsilon_1| + \varrho \|S\| \|\epsilon\|_2^2, \end{aligned} \tag{11}$$

where we have applied the l_1-norm to ϵ and taken into consideration Assumption 2. From the Young inequality, it follows that

$$\begin{aligned} \dot{V} \leq -\epsilon^\intercal \left(\theta S + \Gamma^\intercal S \right) \epsilon - k|\epsilon_1| + \varrho \|S\| \|\epsilon\|_2^2 \\ + \frac{1}{2} \gamma \|S\| |\dot{u}|_\infty \left(|\epsilon_1|^2 + 3|\epsilon_2|^2 \right). \end{aligned} \tag{12}$$

Notice that

$$\frac{1}{2} \gamma \|S\| |\dot{u}|_\infty \left(|\epsilon_1|^2 + 3|\epsilon_2|^2 \right) \leq \vartheta \|S\| \|\epsilon\|_2^2 \tag{13}$$

holds in a region around the origin as big as $\vartheta \in \mathbb{R}_{>0}$, where we choose $\vartheta > \frac{3}{2} \gamma |\dot{u}|_\infty$. From (13) it follows that

$$\dot{V} \leq -\epsilon^\intercal \left(\theta S + \Gamma^\intercal S \right) \epsilon - k|\epsilon_1| + (\varrho + \vartheta) \|S\| \|\epsilon\|_2^2, \tag{14}$$

where $\dot{V} \leq -(\theta - \varrho - \vartheta) V$ holds. Furthermore, it is possible to achieve $\dot{V} \leq -k|\epsilon_1| - \bar{k}|\epsilon_2| \leq -\min\{k, \bar{k}\} V^{1/2}$ in a region around the origin with proper positive constants $(k, \bar{k})$. This means that the observer converges in finite time in such a region. Besides, outside this region, the observer converges exponentially. This ends the proof. □

Remark 1. *Notice that observer* (6) *takes from system* (3) *only the available state z_1. This can be easily seen since $C^\intercal C \epsilon = C^\intercal (\hat{z}_1 - z_1)$, and $C^\intercal C \operatorname{Sgn} \epsilon = C^\intercal \operatorname{sgn} \epsilon_1$ hold.*

IV. Control

Once the estimated hysteresis is available ($\hat{z}_2 = \hat{h}$), we can proceed to control system (Σ, Ω). With that aim, we proceed into a two-step algorithm based on the output-feedback control scheme [22]. The first step is to stabilize the subsystem Ω by using h as a virtual control. The designed virtual control is denoted by h_d. The second step stabilizes the subsystem Σ by finding control u by solving the tracking problem, i.e., finding u such that h converges to virtual control h_d. A scheme of the proposed control approach is depicted in Fig. 2.

A. Control for the subsystem Ω

We take into account the following assumption:

Assumption 3. *The system individual disturbances are bounded:* $|\delta_x| \leq \varrho_1|\tilde{x}|$, *and* $|\delta_h| \leq \varrho_2|e|$, *where* $\tilde{x} = x - x_d$, *and* $e = h - h_d$.

The first result is summarized next.

Proposition 2. *Consider the system* (2), *then, the virtual control*

$$h_d = \frac{1}{B}\left([A - \kappa_1]\tilde{x} + Ax_d - \dot{x}_d + Bd_p u\right) \tag{15}$$

globally asymptotically stabilizes $\{\tilde{x} = 0\}$, *where* $\tilde{x} = x - x_d$, *if* $\kappa_1 > \varrho_1$, *and* $|\delta_x| \leq \varrho_1|\tilde{x}|$ *holds.*

Proof. Please see our previous work [16]. □

B. Nonlinear model predictive control for sub-system Σ

Once we have obtained the desired value $h_d(t)$ for subsystem Ω, we continue to solve the tracking problem for subsystem Σ. With that aim, we propose a nonlinear model predictive control (NMPC) approach responsible to track the desired h_d given by (15) to stabilize system Σ in (1). For it, let us consider that the first time-derivative of the control input u, i.e. $\dot{u}$, is a control variable for (1). In particular, the NMPC must find control $\dot{u}$ in order to $h \to h_d$.

1) NMPC setting: The NMPC can control a system while satisfying a set of given constraints. Usually, such a system is a nonlinear one modeled in discrete time. The NMPC minimizes a predefined cost function by computing: a) a sequence of optimal controls, where only the first control input of the control sequence is applied to the system; and b) the optimal trajectory for the system in question. Both are computed by taking into account the given constraints over a *finite horizon*. The latter process is repeated from the current step to find new controls and a new predicted trajectory.

To solve the NMPC, we have to discretize system dynamics (Σ, Ω). With that aim, we use the well-known forward Euler method with sampling period $T_s = 0.005$ sec.

2) Optimization: The NMPC problem is solved by the sequential quadratic programming (SQP) method used for solving constrained nonlinear optimization problems. Such a method solves problems of the form:

$$\min_x \ f(x), \ \text{subject to } g_1(x) \geq 0, \ g_2(x) = 0. \tag{16}$$

Model predictive control uses the system's model to predict and optimize the control signals in some prediction window called the *horizon*. The latter consists in minimizing, at a sampling time k, a suitably defined cost function with respect to the control sequence $\mathbf{u}_k = (u_k, u_{k+1}, \cdots, u_{k+n_u-1})^T$, where $n_u \geq 1$ is the control horizon.

The cost function to minimize with respect to $\mathbf{u}_k$ is:

$$J(u_k) = \sum_{i=0}^{n_u-1} \left\|u_{(k+1)+i}\right\|_Q^2 + \sum_{i=1}^{n_y} \left\|h_{k+i} - h_{k+i}^d\right\|_R^2, \tag{17}$$

where $n_y \geq 1$ is the prediction horizon; h_{k+i} and $u_{(k+1)+i}$ are, respectively, the predicted outputs and inputs; and h_{k+i}^d denotes the i-th reference output. The term $\|r_i\|_W^2$ denotes the square norm of a vector weighted by a matrix W. In (17) $Q \in \mathbb{R}^{n_u \times n_u}$, and $R \in \mathbb{R}^{n_y \times n_y}$ are diagonal matrices.

3) Constraints: The cost function (17) is subject to the hard constraints given by the discretized system dynamics Σ:

$$\mathbf{h}_{k+1} = f\left(\mathbf{h}_k, \mathbf{u}_k, \mathbf{u}_{k+1}\right). \tag{18}$$

4) NMPC: The NPMC finds the optimal sequence of control inputs u_k by solving the optimization problem:

$$\min_{\mathbf{u}_k} \ J(\mathbf{u}_k, \mathbf{h}_k, n_y, n_u), \tag{19}$$

which leads to the optimal sequence of control inputs $\mathbf{u}_k$. As it is usually done, only the first element u_k is applied to the system. At the next iteration, the minimization problem is restarted, and a new sequence of optimal control inputs is computed. This loop is repeated until the task is achieved.

V. Simulation Results

In this section, we present the conducted simulation experiments showing the closed-loop performance. The simulation is performed in Matlab Simulink.

In the sequel, the units of y, y_d, x and h are in μm, while u is in Volts. The units of the parameters α and d_p are automatically in accordance with these. The initial conditions for the system states are $x(0) = 3$, $h(0) = -2$, and for the observer are set to zero. The parameters of the generalized Bouc-Wen model are [7]: $\beta_1 = 0.0032$, $\beta_2 = 0.0035$, $\beta_3 = -0.0010$, $\beta_4 = -0.0003$, $\beta_5 = -0.0002$, and $\beta_6 = 0.0004$. The parameters for the system Ω are: $A = -\frac{1}{\tau}$, $B = \frac{1}{\tau}$ with $\tau = 0.001s$, and $C = [1, 0]$ (and hence $y_d = x_d$ hereafter). Furthermore, with the aim of showing the control effectiveness under parameter variations, we conducted experiments with three different sets of system parameters, depicted in Tab. I.

TABLE I: Set of parameters used in the simulation.

Parameters set	d_p $(\mu m/V)$	α
No.1	1.0773	0.40648
No.2	1.6	0.9
No.3	10	0.4297

The observer parameter is $\theta = 100$; the gain of the observer is set to $k = 10$. The reference signal is chosen as $x_d = 80 \sin \frac{2\pi}{10} t$ where the frequency is 0.1 Hz. The gain is $\kappa_1 = 500$ for control (15). In all the experiments, the prediction horizon of the NMPC $n_y = 10$, and the control horizon $n_u = 2$; the

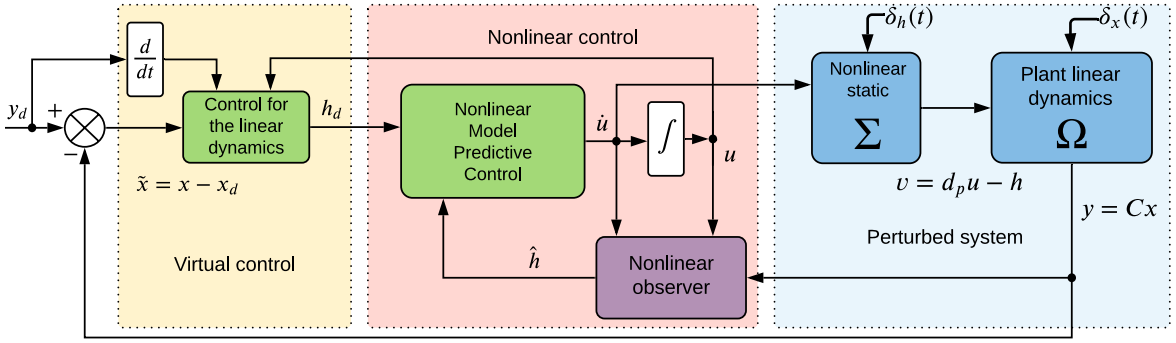

Fig. 2: A diagram showing the closed-loop system consisting of system (Σ, Ω), hysteresis observer (6), and the NMPC with hysteresis desired value designed as in (15).

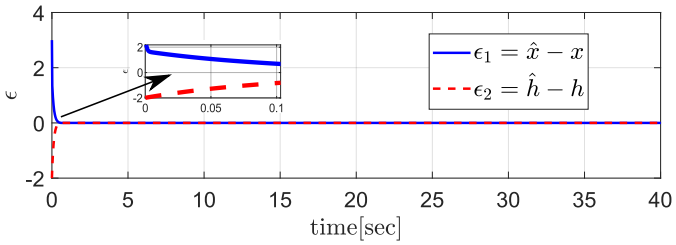

Fig. 3: The convergence of the observer error ϵ to zero.

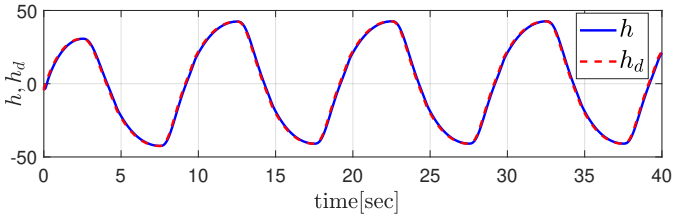

Fig. 4: Hysteresis control. The convergence of the system state h to h_d due to the NMPC.

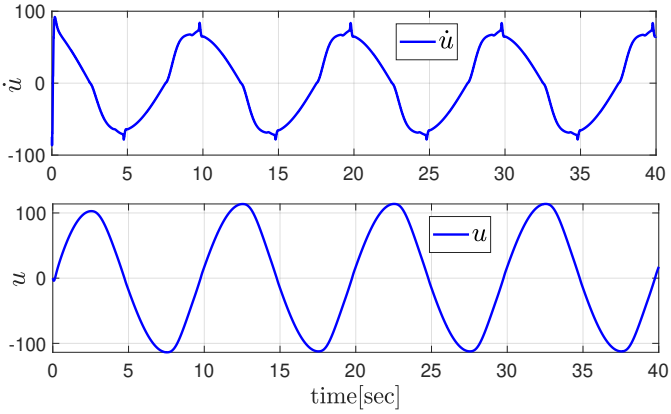

Fig. 5: The control u, and $\dot{u}$, in the NMPC.

weight matrices are set to $Q = \text{diag}\,(0.0001, 0.0001)$, $R = \text{diag}\,(2.0, \ldots, 2.0)$. The values of the matrix R is higher than the ones of Q because we want the error of the output to be more important than the energy terms in the total cost.

Let us consider the simulation with system parameters set No.1 of Tab I. The goal is to track the reference h_d in (15) to stabilize the system Σ in (1) with observer (6) and the proposed NMPC. Fig. 3 shows the observer error evolution $\epsilon = \hat{z} - z$ corresponding to the dynamics of (7). The top row of Fig. 7 shows the convergence of x to x_d. As can be seen, the hysteresis does not affect the convergence. The convergence of h to h_d due to the NMPC is shown in Fig. 4. The Fig. 5 shows the real control input u and its first-time derivative $\dot{u}$.

Besides, we have compared the proposed controller with the open-loop response. For that, we apply a sinusoidal voltage $u(t)$ with a frequency of $0.1Hz$ and amplitude such that the output reaches $80\mu m$. In Fig. 6a, we depict the resulting curve in the (u, y) map. As expected, the actuator has a strong hysteresis when no control is applied. The hysteresis amplitude is $h_{amp} = \frac{h_m}{h_M} \approx \frac{49}{81} = 62\%$ which is strong. Fig. 6b shows the resulting curve from applying a sinusoidal reference y_d of the same frequency and amplitude $80\mu m$ with the proposed approach. As it can be seen, the hysteresis is completely removed. We simulated the closed-loop system for the rest of the parameter set in Tab. I. Fig. 7 shows that the control achieved good performance for all the parameters set. These results highlight that our control is independent of the variability in the parameters of the hysteresis model.

To show the closed-loop system robustness under external disturbances, given by $\delta_x = 30\mu m$ and $\delta_h = 25\sin(t)\,\mu m$, we

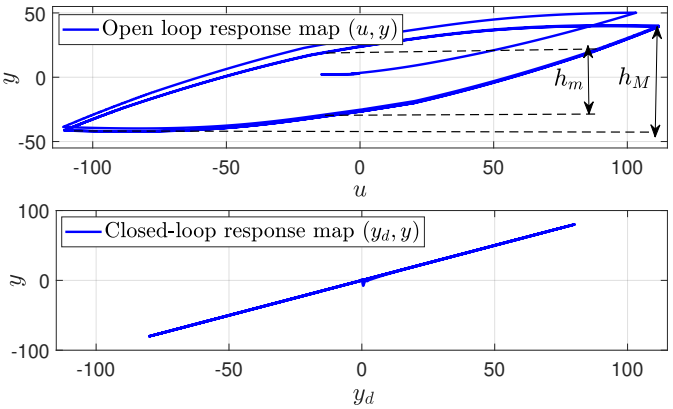

Fig. 6: Input-Output responses: (a) (u, y) map for the open-loop system, and (b) (y_d, y) map for the closed-loop system.

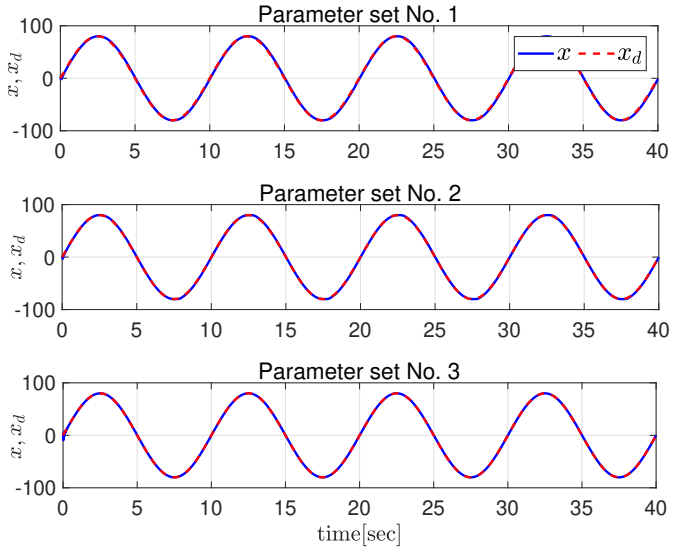

Fig. 7: Input-Output response with set of parameters corresponding to Tab. I.

conduct simulations with the parameter set No. 1 in Tab. I. The system response is depicted in Fig.8. Notice that the open-loop system response is highly disturbed, while in the closed-loop system case, the error due to disturbances is negligible.

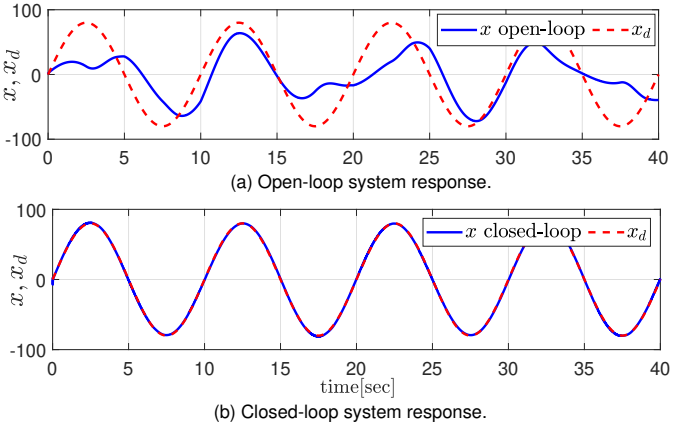

Fig. 8: Input-Output response for the open-loop system (a) and the closed-loop system (b) under the effect of disturbances: $\delta_x = 30\mu m$ and $\delta_h = 25\sin(t)\,\mu m$.

VI. Conclusions

We have presented a robust controller to stabilize a piezoelectrically actuated robotic hand, modeled using the generalized nonlinear Bouc-Wen model, a high nonlinear system that is not differentiable in a finite number of points. Besides, the system takes into account exogenous disturbances.

The proposed control is based on the use of a nonlinear observer that converges in finite time. The observer estimates the hysteresis, which is a variable usually unavailable for feedback. Once we have estimated the hysteresis, we design a controller into two steps: the first step considers the design of a desired hysteresis h_d, while the second finds the control u through a nonlinear model predictive control. The experiments show promising results, and up to our knowledge, this is the first work that solves the problem of stabilization of a piezoelectrically actuated robotic hand, modeled by the generalized nonlinear Bouc-Wen model considering disturbances.

References

[1] M. Rakotondrabe, *Smart materials-based actuators at the micro/nano-scale: characterization, control and applications*. Springer Verlag, New York, Mar. 2013.

[2] M. Mahdavi, M. B. Coskun, and R. Moheimani, "High dynamic range afm cantilever with a collocated piezoelectric actuator-sensor pair," *IEEE Journal of MEMS*, vol. 29, p. 260–267, 2020.

[3] L. Mattos *et al.*, "µralp and beyond: Micro-technologies and systems for robot-assisted endoscopic laser microsurgery," *Frontiers in Robotics and AI, section Biomedical Robotics*, September 2021.

[4] F. J. Salvador *et al.*, "Complete modelling of a piezo actuator last-generation injector for diesel injection systems," *International Journal of Engine Research*, vol. 15, pp. 3–19, 2012.

[5] M. Lok *et al.*, "A low mass power electronics unit to drive piezoelectric actuators for flying microrobots," *IEEE Transactions on Power Electronics*, vol. 33, pp. 3180–3191, 2018.

[6] J. C. Hernandez *et al.*, "Getting started with peas-based flapping-wing mechanisms for micro aerial systems," *Actuators*, vol. 5, p. 14, 2016.

[7] D. Habineza *et al.*, "Multivariable Generalized Bouc-Wen modeling, identification and feedforward control and its application to multi-DoF piezoelectric actuators," *IFAC WC*, pp. 10 952–10 958, 2014.

[8] M. Rakotondrabe, "Bouc-Wen modeling and inverse multiplicative structure to compensate hysteresis nonlinearity in piezoelectric actuators," *IEEE Trans on ASE*, vol. 8, pp. 428–431, Mar. 2011.

[9] ——, "Multivariable classical Prandtl-Ishlinskii hysteresis modeling and compensation and sensorless control of a nonlinear 2-dof piezoactuator," *Nonlinear Dynamics*, Mar. 2017.

[10] M. Al Janaideh *et al.*, "Further results on hysteresis compensation of smart micro-positioning systems with the inverse prandtl-ishlinskii compensator," *IEEE Trans on CST*, vol. 24, pp. 428–439, Jul. 2015.

[11] K. K. Leang, Q. Zou, and S. Devasia, "Feedforward control of piezoactuators in atomic force microscope systems," *IEEE Control Systems Magazine*, vol. 29, pp. 70–82, Mar. 2009.

[12] R. Oubellil *et al.*, "Experimental model inverse-based hysteresis compensation on a piezoelectric actuator," *International Conference on System Theory, Control and Computing*, pp. 186–191, 2015.

[13] J. Escareno *et al.*, "Backstepping-based robust-adaptive control of a nonlinear 2-DOF piezoactuator," *Control Engineering Practice*, vol. 41, pp. 51–71, Mar. 2015.

[14] Y. Shan and K. K. Leang, "Accounting for hysteresis in repetitive control design: Nanopositioning example," *Automatica*, vol. 48, no. 8, pp. 1751–1758, 2012.

[15] M. Ramli *et al.*, "Pseudoextended Bouc-Wen model and adaptive control design with applications to smart actuators," *IEEE Transactions on Control Systems Technology*, vol. 27, no. 5, pp. 51–71, Mar. 2018.

[16] G. Flores and M. Rakotondrabe, "Robust nonlinear control for a piezoelectric actuator in a robotic hand using only position measurements," *IEEE Control Systems Letters*, vol. 6, pp. 872–877, Mar. 2022.

[17] S. Devasia *et al.*, "A survey of control issues in nanopositioning," *IEEE Trans on CST*, vol. 15, pp. 802–823, Mar. 2007.

[18] M. Rakotondrabe, "Modeling and compensation of multivariable creep in multi-dof piezoelectric actuators," *IEEE ICRA, St Paul Minnesota USA*, pp. 4577–4581, 2012.

[19] Y. Al Hamidi *et al.*, "Multi-mode vibration suppression in a multi-dof piezoelectric tube actuator by extending the zero placement input shaping technique," *Actuators*, vol. 5, no. 2, p. 13, 2017.

[20] G. Flores *et al.*, "Output feedback control for a quadrotor aircraft using an adaptive high gain observer," *International Journal of Control, Automation and Systems*, vol. 18, no. 6, pp. 1474–1486, Jun. 2020.

[21] A. E. Rodríguez-Mata, G. Flores *et al.*, "Discontinuous high-gain observer in a robust control UAV quadrotor: Real-time application for watershed monitoring," *Mathematical Problems in Engineering*, vol. 2018, p. 4940360, Nov. 2018, publisher: Hindawi.

[22] G. Flores and M. Rakotondrabe, "Output feedback control for a nonlinear optical interferometry system," *IEEE Control Systems Letters*, vol. 5, no. 6, pp. 1880–1885, 2021.